

On the Light Curves of GRB Afterglows

Ji-Rong Mao ^{*} and Jian-Cheng Wang

Yunnan Observatory, Chinese Academy of Sciences, Kunming 650011
National Astronomical Observatories, Chinese Academy of Sciences, Beijing 100012
United Laboratory of Optical Astronomy, Chinese Academy of Sciences

Received 2001 May 9; accepted 2001 August 31

Abstract We present gamma-ray burst afterglow light curves in X-ray, optical and radio bands for various distributions of accelerated electrons behind the shock. The effects of lateral expansion of the jet and of winds in typical Wolf-Rayet star on the evolution are discussed. The light curves in the radiative case decline more rapidly than those in the adiabatic case. Under the combined effect of jet expansion and wind environment, the light curves have the greatest deviation from those of the standard model. All these results refer to the relativistic phase.

Key words: gamma-rays: burst — hydrodynamics — radiation mechanisms: nonthermal

1 INTRODUCTION

Gamma-ray burst (GRB) afterglows, which are delayed emission in X-ray, optical and radio wavelengths, are usually interpreted as synchrotron radiation from accelerated electrons when a spherical relativistic blast wave sweeps up the external homogeneous medium (Piran 1999; van Paradijs, Konveliotou & Wijers 2000; Cheng & Lu 2001). Based on this standard fireball / blast wave model, many outline calculations of the evolution of GRB afterglows were made (Waxman 1997a, b; Vietri 1997; Sari, Piran & Narayan 1998; Dermer, Böttcher & Chiang 1999, 2000; Granot, Piran & Sari 2000; Kumer & Panaitescu 2000b). However, some authors noted that wind environment should be important for the evolution (Chevalier & Li 1999, 2000; Li & Chevalier 2000; Dai & Lu 1998, 1999, 2000; Panaitescu & Kumar 2000). Some sources are believed to be jetted ejecta, and the corresponding anisotropic model was also discussed analytically and numerically (Rhoads 1997, 1999; Sari, Piran & Halpern 1999; Moderski, Sikora & Bulik 2000; Huang et al. 2000; Frail et al. 2001). The joint effect of jet and wind environment on the GRB afterglows was considered (mészáros 2001) to interpret some observed afterglow data (Kumar & Panaitescu 2000a; Dai & Gou 2000). All of these conditions complicate the evolution of GRB afterglows.

In this paper, we systematically present overall light curves of GRB afterglows and compare the differences arising from different physical conditions. In Section 2, we review the main idea

^{*} E-mail: mjr@cosmos.ynao.ac.cn

of hydrodynamics (Mao & Wang 2001). The synchrotron radiation formula and the relativistic transformation are given in Section 3. In Section 4, we give our results and discuss their physical meaning.

2 HYDRODYNAMICS

The main problem of hydrodynamic evolution for the fireball is how the Lorentz factor $\Gamma(r)$ of the shock evolves with the radius r , measured in the lab frame. There are two basic equations (Blandford & McKee 1976; Chiang & Dermer 1999):

$$\frac{d\Gamma}{dm} = -\frac{\Gamma^2 - 1}{M}, \quad (1)$$

$$\frac{dM}{dr} = \rho(r)A(r)[(\Gamma(r) - 1)(1 - \varepsilon_e) + 1], \quad (2)$$

where M is the total mass, $dm = A(r)\rho(r)dr$ is the rest mass swept-up by the shock in distance dr and $A(r)$ is cross-sectional area. We assume that some fraction ε_e of the kinetic energy is injected directly into non-thermal electrons.

Equation (1) is only suitable for the ultra-relativistic phase. Its result of non-relativistic phase cannot yield the classical Sedov-Taylor solution. The equation of the blast wave is derived more precisely and generally by Huang et al (1999a, b). In this article, we concentrate on the relativistic phase and neglect the non-relativistic phase. So Equation (1) is enough for the relativistic hydrodynamics.

The density of the medium obeys the equation

$$\rho = \rho_0 \left(\frac{r}{r_0}\right)^{-k} = n_0 m_p \left(\frac{r}{r_0}\right)^{-k}, \quad (3)$$

where k is a numerical parameter, m_p the rest mass of proton and $r_0 = (\frac{\sigma_T M_0}{4\pi m_p})^{1/2} \sim 10^{13}$ cm (Piran 1999) is the initial radius when the fireball becomes optically thin to produce gamma-ray bursts. $M_0 \sim 10^{-4} M_\odot$ is the initial mass of the shock shell. From Equations (1) and (2), we have

$$\frac{d\Gamma}{dr} = -\frac{n_0 m_p}{M_0} A(r) \left(\frac{r}{r_0}\right)^{-k} (\Gamma^2 - 1)^{3/2} (\Gamma + 1)^{-\varepsilon_e} (\Gamma_0^2 - 1)^{-1/2} (\Gamma_0 + 1)^{\varepsilon_e}. \quad (4)$$

There is a deceleration radius R_0 defined by

$$M_0 = \int_{r_0}^{R_0} \Gamma_0 A(r) \rho(r) dr, \quad (5)$$

where $\Gamma_0 = 100$ is the initial Lorentz factor. If the medium environment is spherical, then

$$A(r) = 4\pi r^2, \quad (6)$$

and the deceleration radius is given by

$$R_0 = \left[\frac{(3 - k)M_0}{4\pi n_0 m_p \Gamma_0 r_0^k} \right]^{\frac{1}{3-k}}. \quad (7)$$

We define

$$\chi = \frac{r}{R_0}, \quad (8)$$

and Equation (4) can be rewritten as

$$\frac{d\Gamma}{d\chi} = -\frac{(3-k)}{\Gamma_0} \chi^{2-k} (\Gamma^2 - 1)^{3/2} (\Gamma + 1)^{-\varepsilon_e} (\Gamma_0^2 - 1)^{-1/2} (\Gamma_0 + 1)^{\varepsilon_e}. \quad (9)$$

If we take into account the jet expansion of the fireball, then the cross-sectional area of the shock wave is given by

$$A(r) = \Omega_j r^2, \quad (10)$$

where Ω_j is the solid angle of the shock wave. As a result of lateral expansion (Rhoads 1997, 1999) due to the properties of thermodynamics, the value of Ω_j is not constant, rather, it is increasing. The detailed evolution of lateral expansion is discussed by Huang et al (2000a, b). Here, for simplicity, we assume

$$\Omega_j = \left(\frac{r}{r_0}\right)^g \Omega_0, \quad (11)$$

$$\Omega_0 = 2\pi(1 - \cos \theta_0), \quad (12)$$

where g is a numerical parameter and the deceleration radius,

$$R_0 = \left[\frac{(3+g-k)M_0}{\Gamma_0 \Omega_0 n_0 m_p r_0^{k-g}} \right]^{\frac{1}{3+g-k}}. \quad (13)$$

Then we have the equation of the fireball evolution in the case of jet expansion

$$\frac{d\Gamma}{d\chi} = -(3+g-k) \frac{\chi^{g+2-k}}{\Gamma_0} (\Gamma^2 - 1)^{3/2} (\Gamma + 1)^{-\varepsilon_e} (\Gamma_0^2 - 1)^{-1/2} (\Gamma_0 + 1)^{\varepsilon_e}. \quad (14)$$

The differential Equations (9) and (14) can be solved numerically.

3 SYNCHROTRON RADIATION

3.1 Connection with Dynamics

The hydrodynamic evolution of the fireball model primarily determines the properties of the observed light curves of afterglow. However, the electron distribution may give dynamical constraints. In the absence of radiation loss, the distribution of the shock-accelerated electrons behind the blast wave is usually assumed to be a power-law function of electron energy. But radiation loss may affect the electron distribution for GRB afterglows. Three cases are discussed (Dai, Huang & Lu 1999):

(i) For $\gamma_c \leq \gamma_{\min}$

$$\frac{dN'_e}{d\gamma_e} = c_1 \gamma_e^{-(p+1)}, \quad \gamma_{\min} \leq \gamma_e \leq \gamma_{\max}, \quad (15)$$

$$c_1 = \frac{p}{\gamma_{\min}^{-p} - \gamma_{\max}^{-p}} n'_{\text{ele}}. \quad (16)$$

(ii) For $\gamma_{\min} < \gamma_c \leq \gamma_{\max}$

$$\frac{dN'_e}{d\gamma_e} = c_2 \gamma_e^{-p}, \quad \gamma_{\min} < \gamma_e \leq \gamma_c, \quad (17)$$

$$\frac{dN'_e}{d\gamma_e} = c_3 \gamma_e^{-(p+1)}, \quad \gamma_c < \gamma_e < \gamma_{\max}, \quad (18)$$

$$c_2 = c_3/\gamma_c, \quad (19)$$

$$c_3 = \left[\frac{\gamma_{\min}^{1-p} - \gamma_c^{1-p}}{\gamma_c(p-1)} + \frac{\gamma_c^{-p} - \gamma_{\max}^{-p}}{p} \right]^{-1} n'_{\text{ele}}. \quad (20)$$

(iii) For $\gamma_c \geq \gamma_{\max}$

$$\frac{dN'_e}{d\gamma_e} = c_4 \gamma_e^{-p}, \quad c_4 = \frac{p-1}{\gamma_{\min}^{1-p} - \gamma_{\max}^{1-p}} n'_{\text{ele}}. \quad (21)$$

Here, we take $p = 2.5$, $\gamma_{\max} = 4 \times 10^7$ (de Jager et al. 1996; de Jager & Harding 1992). n'_{ele} is the electron number density of shocked material. $\gamma_{\min} = 610\varepsilon_e\gamma$ and $\gamma_c = \frac{6\pi m_e c}{\sigma_T \gamma B'^2 t}$ (Sari, Piran & Narayan 1998) are measured in the comoving frame. γ is the Lorentz factor of the shocked fluid and $\Gamma = \sqrt{2}\gamma$ is measured in the lab frame. In the lab frame, behind the shock, the particle density and the energy per particle are given by $2\Gamma^2 n_0$ and $\Gamma^2 m_p c^2$ (Blandford & McKee 1976). So the magnetic field strength is

$$B = 4(\pi\varepsilon_B m_p n_0)^{1/2} \Gamma^2 c \quad (22)$$

and the critical γ_c is

$$\gamma_c = \frac{6\sqrt{2}\pi m_e c}{\sigma_T \Gamma B^2 t}. \quad (23)$$

The relation between the observed time of a photon and the radius at which it was emitted is given by Sari (1998). The true surface of equal arrival time in the lab frame becomes distorted ellipsoid due to deceleration of the blast wave shell, but this distortion only modifies slightly the radiation flux (Sari 1998; Panaitescu & Mészáros 1998). Here, we assume a photon is emitted from the line of sight of the observer. Then, the relation of the radius r and the arrival time t is (Sari 1997)

$$r = 16\gamma^2 ct = 8\Gamma^2 ct. \quad (24)$$

So, case (i), $\gamma_c \leq \gamma_{\min}$ corresponds to

$$\frac{96\pi m_e c^2}{610\varepsilon_e \sigma_T B^2} \leq r. \quad (25)$$

Case (ii), $\gamma_c > \gamma_{\min}$ corresponds to

$$\frac{96\pi m_e c^2}{610\varepsilon_e \sigma_T B^2} > r. \quad (26)$$

Case (iii), $\gamma_c > \gamma_{\max}$ corresponds to

$$\frac{48\sqrt{2}\pi m_e c^2 \Gamma}{4 \times 10^7 \sigma_T B^2} \geq r. \quad (27)$$

In fact, from numerical results of Equations (9) and (14), we always obtain the result of equation $\frac{48\sqrt{2}\pi m_e c^2 \Gamma}{4 \times 10^7 \sigma_T B^2} < r$. So Equation (27) is untenable and Case (iii) cannot exist.

3.2 Synchrotron Radiation and Relativistic Transformation

After obtaining the modified electron distribution functions, we can calculate their radiation. Here, we concentrate on the relativistic phase and neglect the non-relativistic phase. The power for synchrotron radiation from the accelerated electrons of the shocked medium in the comoving frame is given by

$$j'(\nu') = \frac{dP'}{d\nu'} = \frac{2\sqrt{3}\pi e^2 \nu_L}{c} \int \frac{dN'_e}{d\gamma_e} \left[\frac{\nu}{\nu_c} \int_{\nu/\nu_c}^{\infty} K_{5/3}(t) dt \right] d\gamma_e, \quad (28)$$

where $\nu_L = \frac{1}{2\pi} \frac{eB'}{m_0 c}$ is the Lamor frequency, $\nu_c = \frac{2}{3} \nu_L \gamma_e^2$ and $K_{5/3}(t)$ is Bessel function. There is an approximate expression (Kaplan & Tsytovich 1973):

$$\frac{\nu}{\nu_c} \int_{\nu/\nu_c}^{\infty} K_{5/3}(t) dt = \sqrt{3} \left(\frac{3}{2} \right)^{1/3} \left(\frac{\nu}{\nu_c} \right)^{1/3} e^{-\nu/\nu_c}. \quad (29)$$

The angular distribution of power is

$$\frac{dP'}{d\Omega'} = \frac{1}{4\pi} \int j'(\nu') dV'. \quad (30)$$

If the environment is isotropic, then

$$dV' = 4\pi r^2 \Delta l. \quad (31)$$

The thickness of the blast wave shell Δl is about r/Γ^2 (Blandford & McKee 1976). From particle conservation, we have

$$\Delta l = \frac{r}{6\Gamma^2}. \quad (32)$$

If we take into account jet expansion, then

$$dV' = \Omega_j r^2 \Delta l. \quad (33)$$

Next, we calculate the radiation in the lab frame by relativistic transformation. It is worth noting that the number of accelerated electrons behind the shock is not constant. In Equations (15) and (18), the electron number density of shocked material is given by (Blandford & McKee 1976)

$$n'_{\text{ele}} = 2\Gamma^2 n_0. \quad (34)$$

The frequency and the radiation in the comoving frame can be transformed into the lab frame by (Lind & Blandford 1985)

$$\nu = \delta \nu', \quad (35)$$

$$\frac{dP}{d\Omega} = \delta^3 \frac{dP'}{d\Omega'}, \quad (36)$$

here, δ is the Doppler factor. In the relativistic case,

$$\delta = \frac{1}{\Gamma(1-\beta)} = \frac{\sqrt{1-\beta^2}}{(1-\beta)} = \frac{1+\beta}{\sqrt{1-\beta^2}} \simeq 2\Gamma. \quad (37)$$

So, Equations (33) and (34) can be rewritten as

$$\nu = 2\Gamma \nu', \quad (38)$$

$$\frac{dP}{d\Omega} = (2\Gamma)^3 \frac{dP'}{d\Omega'}. \quad (39)$$

4 RESULTS AND DISCUSSION

In our work, the evolution of the light curve is affected by four parameters: ε_e , ε_B , k and g . ε_e measures the fraction of the total thermal energy going into random motions of the electrons. In the framework of the fireball model for GRBs, the two classes which are interpreted as radiative and adiabatic regimes are well defined by X-ray observation (Boër & Gendre 2000). From the hydrodynamics of the blast wave shell, there are also at least two regimes: adiabatic and radiative. The case $\varepsilon_e = 1$ is the radiative regime of hydrodynamics for the blast wave shell because the electrons can tap all of the available internal energy of the blast wave shell. Conversely, we take $\varepsilon_e = 0.1$ and expect the dynamics of the blast wave to be in the adiabatic regime. If the coupling between the magnetic field and particles is weak, the blast dynamics should be intermediate between radiative and adiabatic. The parameter ε_B measures the ratio of the magnetic field energy to the total thermal energy. $\varepsilon_B = 1$ means a purely magnetic fireball (Mészáros, Laguna & Rees 1993). In principle, ε_B will change with time and depends on complicated plasma physics. Here, we assume that the magnetic field is randomly oriented in space. So we keep it as a free parameter. In this paper, we take $\varepsilon_B = 0.01$ and $\varepsilon_B = 0.5$. The expression of Equation (3) presents a typical wind environment of Wolf-Rayet star if the parameter $k = 2$. The effect of Wolf-Rayet star wind on the afterglows of GRB is well discussed (Ramirez-Ruiz et al. 2000). The parameter g in Equation (11) measures the degree of lateral expansion in the jet. Here, we take $g = 2$ and the lateral expansion should be important to the evolution of the light curves. These four parameters correspond to different physical conditions. Varying these parameters gives different patterns of light curves in X-ray, optical and radio bands.

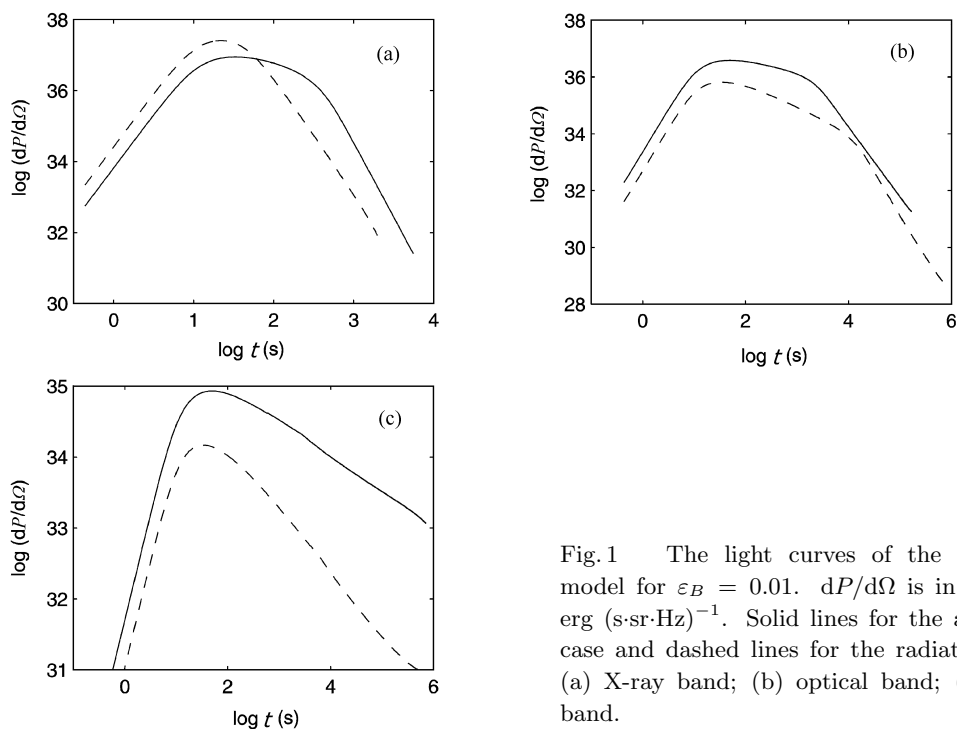


Fig.1 The light curves of the standard model for $\varepsilon_B = 0.01$. $dP/d\Omega$ is in units of $\text{erg} (\text{s}\cdot\text{sr}\cdot\text{Hz})^{-1}$. Solid lines for the adiabatic case and dashed lines for the radiative case. (a) X-ray band; (b) optical band; (c) radio band.

Figure 1 displays the light curves for the standard model in X-ray, optical and radio wavelengths, and the difference between the adiabatic and radiative cases. The evolution in the radiative case is more rapid than in the adiabatic case because the electrons in the former tap more thermal energy to radiate. Figure 2 shows the different light curves in the radiative case between $\varepsilon_B = 0.5$ and $\varepsilon_B = 0.01$, also in X-ray, optical and radio bands, respectively. Since the case of $\varepsilon_B = 0.5$ has more magnetic energy, it has more powerful radiation flux than the case of $\varepsilon_B = 0.01$. Figure 3 shows the light curves in the wind environment in the radiative case, in X-ray, optical and radio bands, respectively. Here, we take $\varepsilon_B = 0.01$. Comparing with Fig.1, the declining of the light curves in the wind environment is more rapid than in the standard model because the blast wave shell sweeps up more dense medium matter in the wind environment. Figure 4 shows the light curves in the radiative case for the standard model, with jet expansion and under the joint effect of jet and wind environment. Here, we also take $\varepsilon_B = 0.01$. From these figures, we find that jet expansion exerts an important effect on the light curves. The light curves under the joint effect of jet expansion and wind environment deviate most from those of the standard model.

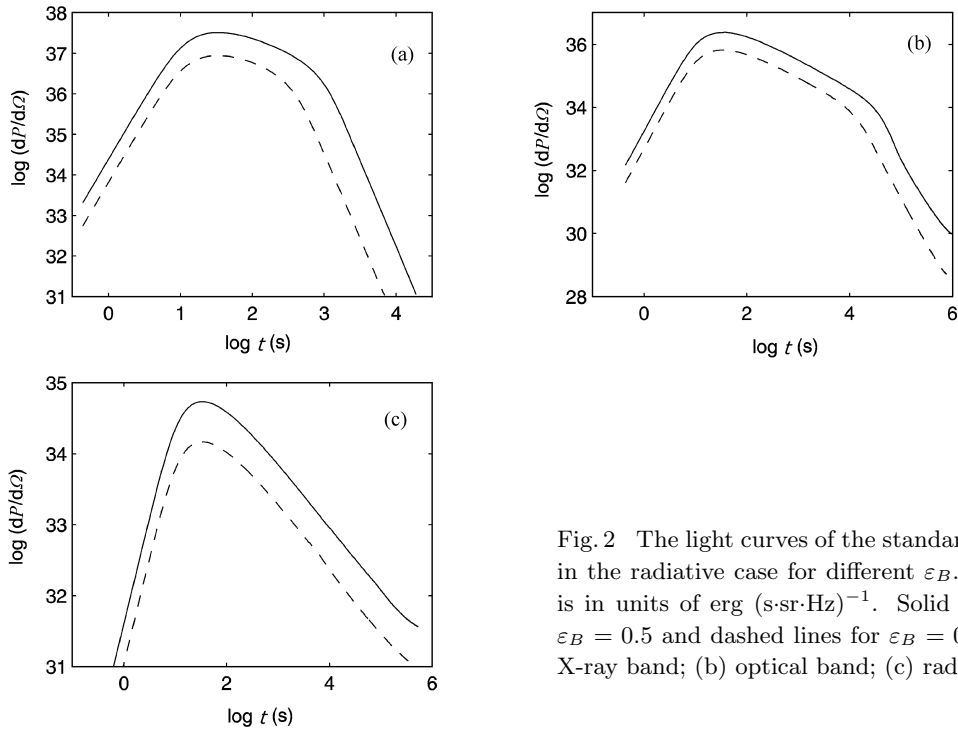


Fig. 2 The light curves of the standard model in the radiative case for different ε_B . $dP/d\Omega$ is in units of $\text{erg} (\text{s}\cdot\text{sr}\cdot\text{Hz})^{-1}$. Solid lines for $\varepsilon_B = 0.5$ and dashed lines for $\varepsilon_B = 0.01$. (a) X-ray band; (b) optical band; (c) radio band.

We have given a detailed description of GRB afterglow light curves. Our conclusions are summarized as follows.

- (1) The light curves evolve faster in the radiative case than in the adiabatic case.
- (2) A smaller value of ε_B corresponds to a smaller radiation flux.
- (3) The light curves decline faster in the wind environment than in the standard model.
- (4) The light curves under the joint effect of jet expansion and wind environment deviate the most from those of the standard model.

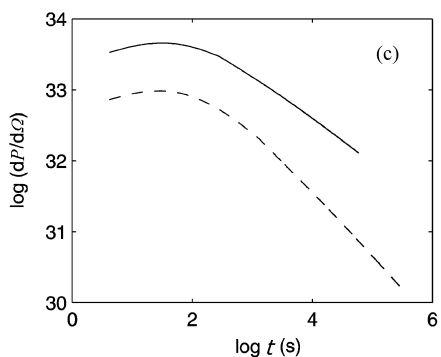
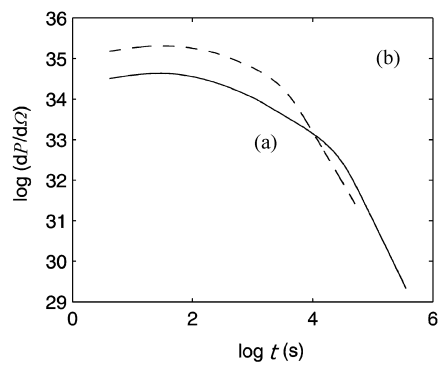
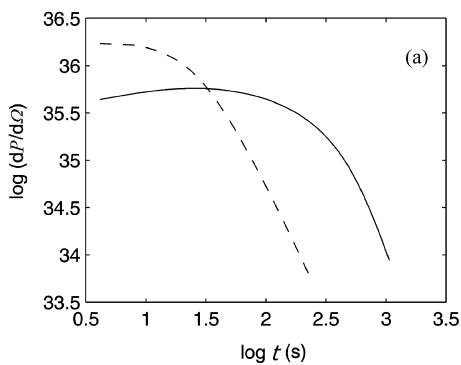


Fig. 3 The light curves of wind environment ($k = 2$) with $\varepsilon_B = 0.01$. $dP/d\Omega$ is in units of $\text{erg (s}\cdot\text{sr}\cdot\text{Hz)}^{-1}$. Solid lines for the adiabatic case and dashed lines for the radiative case. (a) X-ray band; (b) optical band; (c) radio band.

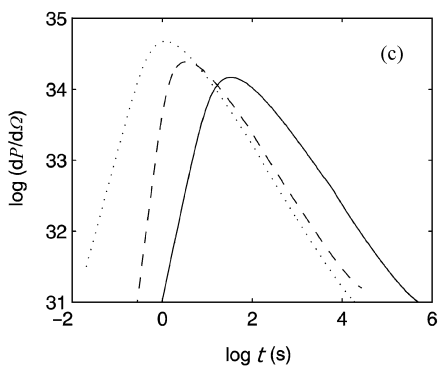
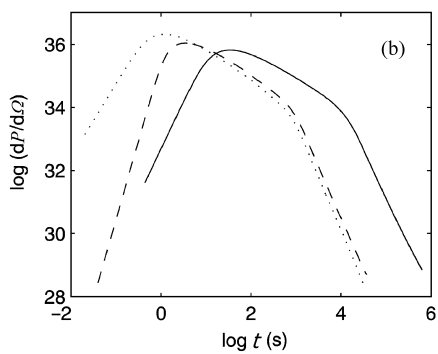
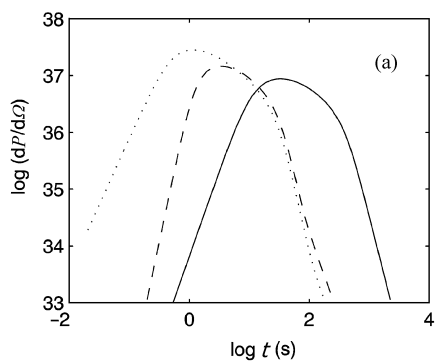


Fig. 4 Comparison of the light curves in various environments in the radiative case with $\varepsilon_B = 0.01$. $dP/d\Omega$ is in units of $\text{erg (s}\cdot\text{sr}\cdot\text{Hz)}^{-1}$. Solid lines for the standard model, dashed lines for jet expansion ($g = 2$) and dotted lines taking into account the joint effect of jet expansion ($g = 2$) and wind environment ($k = 2$). (a) X-ray band; (b) optical band; (c) radio band.

Though we calculated the light curves of GRB afterglows in the relativistic phase, we note the importance of non-relativistic phase in the evolution of GRB afterglow. Huang et al. (1998) discussed the evolution of GRB afterglow from ultra-relativistic to non-relativistic phase. The steepening of the late optical afterglow decay may be caused by the shock having evolved from a relativistic to a non-relativistic phase in a dense medium (Dai & Lu 1999). The unusual optical afterglow of GRB000301c may arise from a non-relativistic shock with energy injection (Dai & Lu 2001). The isotropic gamma-ray energy is released by the central engine. However, this kind of energy could grossly overstate the true gamma-ray energy release if the expansion is not spherical. For example, through observation of the steep optical light curve, GRB 990510 (Harrison et al. 1999) and GRB 991216 (Halpern et al. 2000) are considered to be evidence for jet. Nearly all the discussion on jet effects assumed a conical geometry; however, Cheng, Huang & Lu (2001) have studied the GRB afterglows from a cylindrical jet. Recently, radiative hydromagnetic shocks in relativistic outflow sources are discussed (Granot & Königl 2001). Thus, the non-relativistic phase of blast wave shock, the geometry of the jet and relativistic hydromagnetic dynamics should be comprehensively studied in order to go further on the evolution of GRB afterglows.

Acknowledgements We would like to thank the anonymous referee for useful comments. This work is supported by National Observatories grants (99-5102CA), Chinese Academy of Sciences (CAS). The research is subsidized by Special Funds for Major State Research Projects (973 Projects).

References

- Blandford R. D., McKee C. F., 1976, *Phys. Fluids*, 19, 1130
Boër M., Gendre B., 2000, *A&A*, 361, L21
Cheng K. S., Lu T., 2001, *CJAA*, 1, 1
Cheng K. S., Huang Y. F., Lu T., 2001, *MNRAS*, 325, 599
Chevalier R. A., Li, Z.-Y., 1999, *ApJ*, 520, L29
Chevalier R. A., Li Z.-Y., 2000, *ApJ*, 536, 195
Chiang J., Dermer C. D., 1999, *ApJ*, 512, 699
Dai Z. G., Huang Y. F., Lu T., 1999, *ApJ*, 520, 634
Dai Z. G., Lu T., 1998, *MNRAS*, 298, 87
Dai Z. G., Lu T., 1999, *ApJ*, 519, L155
Dai Z. G., Lu T., 2000, *ApJ*, 537, 803
Dai Z. G., Lu T., 2001, *A&A*, 367, 501
Dai Z. G., Gou L. J., 2001, 552, 72
de Jager O. C. et al., 1996, *ApJ*, 457, 253
de Jager O. C., Harding A. K., 1992, *ApJ*, 4396, 161
Dermer C. D., Böttcher M., Chiang J., 1999, *ApJ*, 514, L49
Dermer C. D., Böttcher M., Chiang J., 2000, *ApJ*, 537, 255
Frail D. A. et al., 2001, preprint (astro-ph/0102282)
Granot J., Piran T., Sari R., 2000, *ApJ*, 534, L163
Granot J., Königl A., preprint (astro-ph/0103108)
Halpern J. P. et al., 2000, *ApJ*, 543, 697
Harrison F. A. et al., 1999, *ApJ*, 523, L121
Huang Y. F., Dai Z. G., Lu, T., 1998, *A&A*, 336, L69
Huang Y. F., Dai Z. G., Lu T., 1999a, *MNRAS*, 309, 513
Huang Y. F., Dai Z. G., Lu T., 1999b, *Chinese Physics Letters*, 16, 775

- Huang Y. F. et al., 2000a, ApJ, 543, 90
Huang Y. F. et al., 2000b, MNRAS, 316,943
Kaplan S. A., Tsytovich V. N., 1973, Plasma Astrophysics, Oxford: Pergamon Press
Kumar P., Panaitescu A., 2000a, ApJ, 541, L9
Kumar P., Panaitescu A., 2000b, ApJ, 541, L51
Li Z.-Y., Chevalier R. A., 2001, ApJ, 551, 940
Lind K. R., Blandford R. D., 1985, ApJ, 295, 358
Mao J. R., Wang J. C., 2001, CJAA, 1(4), 349
Mészáros P., 2001, Science, 291, 79
Mészáros P., Laguna P., Rees M. J., 1993, ApJ, 415, 181
Moderski R., Sikora M., Bulik T., 2000, ApJ, 529, 151
Panaitescu A., Mészáros P., 1998, ApJ, 493, L31
Panaitescu A., Kumar P., 2000, ApJ, 543, 66
Piran T., 1999, Phys. Rep., 314, 575
Ramirez-Ruiz E. et al., preprint (astro-ph/0012396)
Rhoads J. E., 1997, ApJ, 487, L1
Rhoads J. E., 1999, ApJ, 525, 737
Sari R., 1997, ApJ, 489, L37
Sari R., 1998, ApJ, 494, L49
Sari R., Piran T., Narayan R., 1998, ApJ, 497, L17
Sari R., Piran T., Halpern J. P., 1999, ApJ, 519, L17
van Paradijs J., Kouveliotou C., Wijers, R. A. M. J., 2000, ARA&A, 38, 379
Vietri M., 1997, ApJ, 478, L9
Waxman E., 1997a, ApJ, 485, L5
Waxman E., 1997b, ApJ, 489, L33